



CHORUS

This is the accepted manuscript made available via CHORUS. The article has been published as:

Stretched Exponential Relaxation of Glasses at Low Temperature

Yingtian Yu, Mengyi Wang, Dawei Zhang, Bu Wang, Gaurav Sant, and Mathieu Bauchy

Phys. Rev. Lett. **115**, 165901 — Published 15 October 2015

DOI: [10.1103/PhysRevLett.115.165901](https://doi.org/10.1103/PhysRevLett.115.165901)

Stretched Exponential Relaxation of Glasses at Low Temperature

Yingtian Yu,¹ Mengyi Wang,¹ Dawei Zhang,¹ Bu Wang,¹ Gaurav Sant,^{2,3} and Mathieu Bauchy^{1,*}

¹*Physics of Amorphous and Inorganic Solids Laboratory (PARISlab),
Department of Civil and Environmental Engineering,
University of California, Los Angeles, CA, USA*

²*Laboratory for the Chemistry of Construction Materials (LC²),
Department of Civil and Environmental Engineering,
University of California, Los Angeles, CA, USA*

³*California Nanosystems Institute (CNSI), University of California, Los Angeles, CA, USA*

(Dated: September 11, 2015)

The question of whether glass continues to relax at low temperature is of fundamental and practical interest. Here, we report a novel atomistic simulation method allowing us to directly access the long-term dynamics of glass relaxation at room temperature. We find that the potential energy relaxation follows a stretched exponential decay, with a stretching exponent $\beta = 3/5$, as predicted by Phillips' diffusion-trap model. Interestingly, volume relaxation is also found. However, it is not correlated to the energy relaxation, but is rather a manifestation of the mixed alkali effect.

PACS numbers: 65.60.+a, 62.40.+i, 81.05.Kf

While it is indeed commonly believed that, as frozen supercooled liquids, glasses should continue to flow over the years (e.g. in the case of the stained-glass windows of medieval cathedrals [1, 2]), the dramatic increase of their viscosity below the glass transition temperature T_g suggests, on the contrary, that their relaxation time is on the order of 10^{32} years at room temperature [3]. However, a recent study conducted by Mauro *et al.* [4] reported the intriguing dynamics of the relaxation of a commercial Corning[®] Gorilla[®] Glass at room temperature, over 1.5 years. Fused silica [5], sodium silicate [6], and metallic glasses [7] were also reported to show an appreciable relaxation over time. More generally, the relaxation of glasses at low temperature is known as the "thermometer effect", originating from the fact that, in the 19th century, thermometers made of alkali lime silicate glass were experiencing gradual changes of dimension over time, making them inaccurate [8, 9].

As it cannot be described as a viscous process, the physical origin of such room temperature relaxation remains unclear. However, the shape of the relaxation function contains valuable information to discriminate between the different proposed models. In particular, Mauro *et al.* observed that the volume of the relaxing Gorilla[®] Glass followed a stretched exponential decay function [4], with a stretching exponent $\beta = 3/7$, which, interestingly, is the value predicted by the Phillips diffusion-trap model for a relaxation dominated by long-range pathways [10]. Understanding and predicting the relaxation dynamics of glasses has important practical applications, e.g. for optical fibers [11], substrate glass for liquid crystal displays [12], and chemically strengthened cover glass for smartphones and tablets [13].

Here, based on molecular dynamics (MD) simulations, we investigate the atomistic origin of the relaxation of realistic alkali aluminosilicate glasses at temperature far

below T_g . As traditional MD is unable to reproduce year-long relaxations, we introduce a novel artificial relaxation method based on cyclic stress perturbations. The potential energy of the simulated glasses is found to follow a stretched-exponential decay function, with a stretching exponent $\beta = 3/5$, characteristic of systems dominated by short-range forces [10]. On the contrary, the volume relaxation appears composition-specific and strongly correlated with the dynamics of the alkali atoms.

For this study, we simulated a 2991 atoms mixed potassium sodium aluminosilicate glass (denoted KNAS hereafter), of composition $(\text{K}_2\text{O})_8(\text{Na}_2\text{O})_8(\text{Al}_2\text{O}_3)_9(\text{SiO}_2)_{75}$, which we expect to be representative of that of the per-alkaline Corning[®] Gorilla[®] Glass used in Ref. [4]. In addition, in order to evaluate the effect of the mixed alkali effect on relaxation, we simulated a similar single alkali glass (denoted NAS hereafter) of composition $(\text{Na}_2\text{O})_{16}(\text{Al}_2\text{O}_3)_9(\text{SiO}_2)_{75}$. All MD simulations are performed with the LAMMPS package [14], using the well-established Teter potential [15–18] and an integration time-step of 1 fs. Coulomb interactions were evaluated by the Ewald summation method, with a cutoff of 12 Å. The short-range interaction cutoff was chosen at 8.0 Å. Liquids were first generated by placing the atoms randomly in the simulation box. The liquids were then equilibrated at 5000 K in the NPT ensemble (constant pressure) for 1 ns, at zero pressure, to assure the loss of the memory of the initial configuration. Glasses were formed by linear cooling of the liquids from 5000 to 300 K with a cooling rate of 1 K/ps in the NPT ensemble at zero pressure. **Two additional coolings at 0.1 and 0.01 K/ps were performed for the KNAS glass to ensure that the cooling rate does not affect significantly the shape of its relaxation. It should be noted that, as described by the heat transfer model proposed by Zasadzinski [19], such cooling rates for nanometric systems are comparable to typical exper-**

imental cooling rates for macroscopic samples [20]. The obtained glasses were eventually relaxed for an additional 1 ns in the NPT ensemble at 300 K and zero pressure. A detailed structural analysis of the simulated glasses can be found in Ref. [18].

Traditional MD simulations are usually limited to a few nanoseconds, which prevents one from using them to predict long-term relaxation at low temperature. On the other hand, kinetic Monte-Carlo simulations like ART [21] offer an attractive alternative to perform simulations up to a few seconds, but their application to alkali silicate is challenging due to the high mobility of the alkali atoms, which results in a huge number of small energy barriers to compute. Since a direct simulation of relaxation dynamics is, at this point, unachievable, we developed a new method to simulate an artificial relaxation.

This method is inspired by the artificial aging or rejuvenation observed in granular materials subjected to vibrations [22, 23]. Small vibrations induce a compaction of the material, that is, they make the system artificially age. On the other hand, large vibrations randomize the grain arrangements, which decreases the overall compactness and, therefore, make the system rejuvenate. Similar ideas, relying on the energy landscape approach [24, 25], have been applied to amorphous solids, based on the fact that small stresses deform the energy landscape undergone by the atoms. This can result in the removal of some energy barriers existing at zero stress, thus allowing atoms to jump over them in order to relax to lower energy states (see the schematic representation in Fig. 1). This transformation is irreversible as, once the stress is removed, the system remains in its "aged" state. On the contrary, large stresses move the system far from its initial state, which eventually leads to rejuvenation, similar to thermal annealing [26, 27]. As such, several experimental and simulation studies reported that glasses can undergo overaging or rejuvenation, when subjected to small or large shear stresses, respectively [24–32]. The novel method presented here is based on a succession of many of such stress perturbations, inducing successive small relaxations of the system.

In practice, a glass initially relaxed at zero pressure is subjected to athermal stress perturbations cycles. Each perturbation cycle consists, successively, of (1) an hydrostatic compressive stress $-\sigma_0$ and (2) an hydrostatic tensile stress σ_0 . Therefore, the average stress remains zero over each cycle. During both of the phases (1) and (2), a volume-variant energy minimization is performed, in which the positions of the atoms and the volume/shape of the simulation box are updated in an iterative process, in order for the system to achieve simultaneously both an energy minimum for the potential energy of the atoms U and a stress σ close to $\pm\sigma_0$. This combined optimization is performed by minimizing a fictitious energy $E_{\text{fic}} = U + E_{\text{strain}}$, where U is the potential energy and E_{strain} a strain energy expression proposed

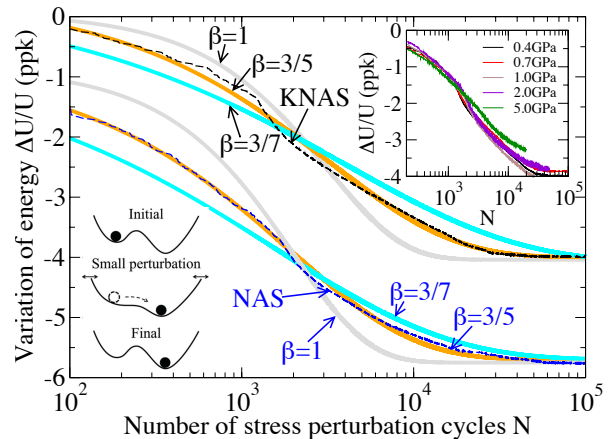


FIG. 1. (color online). Relative variation of the potential energy (stabilization) of the simulated mixed potassium sodium aluminosilicate (KNAS) and sodium aluminosilicate (NAS) glasses, with respect to the number of stress perturbation cycles applied N (with an stress amplitude of 0.4 GPa). For better clarity, the curve obtained for the NAS glass is shifted by -1 . The simulated data are fitted by stretched exponential decay functions with different stretching exponents β (solid lines). A direct fit provides $\beta = 0.602 \pm 0.018$ and 0.606 ± 0.011 for KNAS and NAS, respectively. The inset shows the relative variation of the potential energy of the simulated KNAS glass, for different amplitudes of stress perturbations. The cartoon on the bottom-left is a schematic representation of a strain-induced disappearance of energy barrier. The W curves represent the potential energy between two metastable equilibrium states, and the circles represent the state of the system. The arrow corresponds to a strain-activated jump of the system towards the more stable equilibrium state.

by Parrinello and Rahman [33]. Hence, during each cycle, the system is allowed to jump over energy barriers, with a roughly constant activation energy on the order of E_{strain} . According to transition state theory [34], each cycle should roughly correspond to a constant time of about $\Delta t = \nu_0^{-1} \exp(E_{\text{strain}}/k_B T)$, where ν_0 is a characteristic frequency of attempt, k_B the Boltzmann constant, and T the temperature [35]. Therefore, the relaxation observed with respect to the number of stress perturbations cycles applied N should be representative of the relaxation versus time t , with a converting factor $t = N \Delta t$.

Figure 1 shows the relative variation of the potential energies of the KNAS and NAS glasses, with respect to the number N of stress perturbation cycles applied, with an amplitude $\sigma_0 = 0.4$ GPa. Note that this amplitude remains low as compared to the yield stress in tension (4.4 GPa). As expected, the stress perturbations allow the system to relax towards lower energy states. This stabilization is gradual and about 10^5 of such cycles are needed for the potential energy to plateau. Eventually, a significant decrease of energy (around 0.4%) is achieved. We note that the energy relaxation profile appears to be very similar for the KNAS and NAS glasses. The influ-

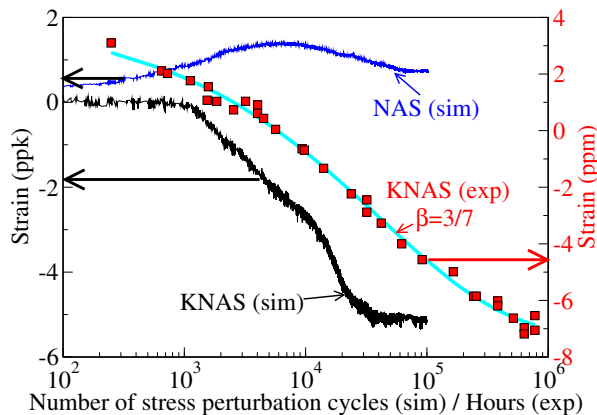


FIG. 2. (color online). Linear strain (compression when negative) observed during the low temperature relaxation of the simulated mixed potassium sodium aluminosilicate (KNAS) and sodium aluminosilicate (NAS) glasses (left axis) with respect to the number of stress perturbation cycles applied N . Simulated results are compared to the experimental measurement of the room temperature compaction of a commercial KNAS glass (right axis) with respect to the time of relaxation [4]. Experimental data are fitted by a stretched exponential decay function (solid line) with a stretching exponent $\beta = 3/7$. Horizontal arrows indicate which axis to refer to.

ence of σ_0 was assessed by performing similar simulations with $\sigma_0 = 0.7, 1, 2,$ and 5 GPa. As shown in the inset of Fig. 1, no significant change of the shape of the energy relaxation is observed at low σ_0 . Therefore, the relaxation dynamics does not depend on the choice of σ_0 . However, the energy starts to decrease more slowly for $\sigma_0 = 5$ GPa, which suggests that, for stresses beyond the yield point, the system is slightly rejuvenated at each cycle, or deviates from the path it would follow upon spontaneous aging. In the following, we keep $\sigma_0 = 0.4$ GPa. Note that accelerated aging techniques, as implemented in previous works [25], have been shown to be potentially non equivalent to spontaneous aging. However, we made sure that the present protocol predicts a realistic relaxation by checking that, starting from a system instantly quenched from the supercooled liquid state, for low stress perturbations, its relaxed states remained on the equilibrium path of the (density, energy) configurational space, as explored by the supercooled liquid at different temperatures. Note that this does not remain true for stress perturbations larger than the yield stress. Overall, this result constitutes the first direct simulation of the relaxation of a glass at low temperature, to the best of our knowledge.

Interestingly, the volume of the glasses does not remain constant through the relaxation procedure. As shown in Fig. 2, the simulated KNAS glass shows a gradual compaction with respect to the number of stress perturbation cycles applied, eventually achieving a final linear strain of about -0.5% . As the average applied stress

remains zero, this compaction cannot be explained by elastic deformations. We note that the extent of the compaction is higher in the present simulation than observed experimentally [4]. This discrepancy is likely to arise from the cooling rate used in simulation, which is much higher than the ones typically achieved experimentally, and from the different compositions of the glasses. However, as shown in Fig. 2, the general trend of the volume relaxation is remarkably fairly similar to that observed experimentally.

The origin of the densification of the Gorilla[®] Glass and, more generally, of the thermometer effect, has been attributed to the mixed alkali effect (MAE) [8, 9]. An MAE is generally observed in silicate or borate glasses containing at least two different network modifying alkali oxides AO_2 and BO_2 . It manifests by a strong non linear evolution of the transport properties with respect to the fraction A/B . Here, the compaction of the KNAS glass can be clearly attributed to the MAE. Indeed, as shown in Fig. 2, the volume of the single alkali NAS glass features a completely different trend, remaining fairly constant over time. This result is consistent with the observation that single alkali-containing Gorilla[®] Glass 2 and 3 do not show any discernable volume relaxation [4]. These results highlight the fact that volume relaxation is not an intrinsic feature of glass, but strongly depends on composition. On the contrary, based on the present results, energy relaxation appears to be more general and, therefore, more relevant to characterize the intrinsic dynamics of glass relaxation.

Indeed, the general shape of the relaxation curve of the potential energy is of fundamental importance as it manifests from the topology of the relaxation process [36]. Glass relaxation behaviors are generally found to follow a stretched exponential decay function $f(t)$ [37]:

$$f(t) = \exp(-(t/\tau)^\beta) \quad (1)$$

where τ is the relaxation time, and β a dimensionless stretching exponent satisfying $0 < \beta < 1$. The case $\beta = 1$ corresponds to a simple exponential decay. The diffusion-trap model from Phillips [10], based on diffusion of excitations to randomly distributed traps, predicts that a theoretical value for the stretching exponent $\beta = d^*/(d^* + 2)$, where d^* is the effective dimensionality of the channels along which the excitations diffuse in the configuration space. This is described as $d^* = fd$, where d is the dimensionality of the system (3 for structural glasses), and f is the proportion of the active channels of relaxation. Hence, when all the channels are active ($f = 1$), one gets $\beta = 3/5$. When only long-range channels are active, by assuming an equipartitioning of the short- and long-range contributions ($f = 1/2$), the model predicts $\beta = 3/7$. It should be noted that this model only applies to perfectly homogeneous glasses, that is, featuring homogeneously distributed excitations and

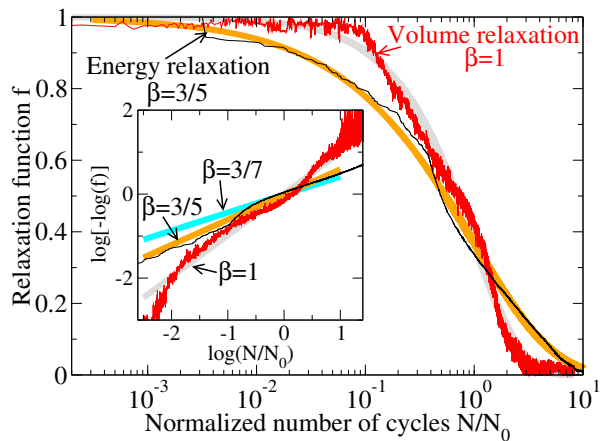


FIG. 3. (color online). Relaxation function f for the energy and volume, computed during the relaxation of the simulated mixed potassium sodium aluminosilicate (KNAS) glass, with respect to the normalized number of stress perturbation cycles applied N/N_0 (see text). The computed data are fitted with stretched exponential decay functions, with stretching exponents $\beta = 3/5$ and 1 for the energy and the volume, respectively. The inset shows $\log(-\log(f))$ with respect to $\log(N/N_0)$, for the energy and volume, whose slope is equal to β . Solid lines with the slopes $\beta = 3/7$, $3/5$, and 1 are added for comparison.

traps. However, unless special care in sample preparation is taken, real-world glasses are likely to show some degree of micron-scale heterogeneity (impurities, partial crystallization, phase separation, partial hydration, local coordination defects, internal stress, etc.) [38, 39]. Such inhomogeneous glasses would therefore feature β exponents that deviate from the predicted values [10, 40].

As shown in Fig. 2, the experimental volume relaxation of the Gorilla[®] Glass was found to follow such a stretched exponential decay function, with a relaxation time $\tau = 27.6$ days and a stretching exponent $\beta = 3/7$, attributed to a relaxation dominated by long-range pathways. Interestingly, the energy relaxation predicted by the present simulations also features a stretched exponential decay, with an equivalent relaxation time $\tau = N_0 \Delta t$, with $N_0 = 3200$ and 1300 for the KNAS and NAS glasses, respectively. This allows us to roughly evaluate Δt , the fictitious time elapsed during each stress perturbation cycle, to be on the order of 10 min. However, as shown in Fig. 1, we unambiguously find a stretching exponent $\beta = 3/5$, which, as mentioned previously, corresponds to the situation in which all the relaxation channels are active [10], which is typically observed for the stress relaxation in glasses [36, 41]. We note that the $\beta = 3/5$ factor offers a good fit, both for the KNAS and NAS glasses, which suggests that it does not depend on changes of composition.

Surprisingly, as shown in Fig. 3, the energy and volume relaxations of the KNAS glass do not show the same

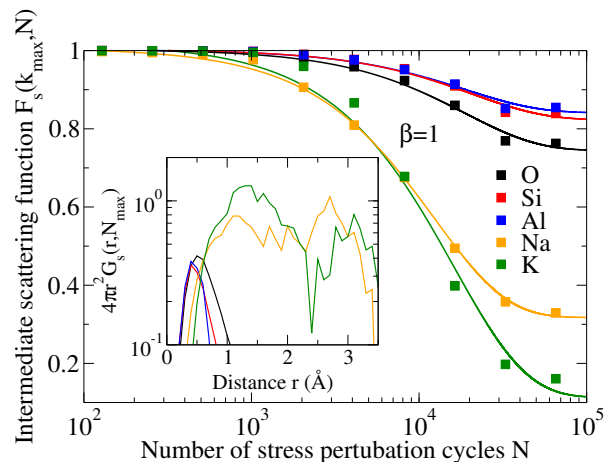


FIG. 4. (color online). O, Si, Al, Na, and K intermediate scattering function $F_s(k, N)$ (computed at k_{\max} , the position of the first peak of the structure factor) of the simulated potassium sodium aluminosilicate (KNAS) glass with respect to the number of stress perturbation cycles applied N . The simulated data are fitted by simple exponential decay functions ($\beta = 1$, solid lines). The inset shows the self-part of the van Hove correlation function $4\pi r^2 G_s(r, N)$ for O, Si, Al, Na, and K, with respect to the distance r , computed at $N_{\max} = 2^{16}$ cycles.

shape. First, we find $N_0 = 3200$ and 12000 for the energy and volume, respectively, suggesting a slower relaxation for the volume than for the energy. Second, the volume relaxation actually follows a simple (that is, not stretched) relaxation decay function. As shown in the inset of Fig. 3, this difference of stretching exponent can be clearly established by plotting $\log(-\log(f))$ versus $\log(N/N_0)$, whose slope is equal to β . This result suggests that energy and volume relax in a fundamentally different way. More specifically, the relaxation of energy can be explained by the diffusion-trap model with all relaxation channels being active [10], whereas the relaxation of volume, showing a simple exponential relaxation, can be explained by a simple two-state model [42].

In order to elucidate the origin of the simple exponential decay for the volume, we investigated the relaxation dynamics of each atomic species by calculating the intermediate scattering function (ISF) $F_s(k, N)$, computed at k_{\max} , the position of the first peak of the structure factor [43]. Interestingly, the ISF of Na and K atoms follow a trend similar to that of the volume relaxation. Indeed, as shown in Fig. 4, it can be fitted by a simple exponential decay function ($\beta = 1$) and show relaxation times similar to that of the volume relaxation (e.g., $N_0 = 11900$ for Na atoms, as compared to 12000 for the volume relaxation). This clearly establishes that the volume relaxation observed in mixed alkali aluminosilicate glasses arises from the relaxation dynamics of the alkali atoms. The self part of the van Hove correlation function, shown in the inset of

Fig. 4, shows that this relaxation of the alkali atoms consists of jumps, with a typical hopping distance of around 3 Å [44–46]. On the contrary, the network former atoms show very limited motion, lower than 1 Å. This highlights the fact that the volume relaxation is not correlated to the viscosity of the glass network, but rather to the dynamics of the alkali modifiers only. The fact that, due to the MAE effect, this dynamics strongly depends on the composition of the glass may explain the discrepancy of stretching exponent between the simulation and experimental results.

Featuring a stressed exponential decay function with $\beta = 3/5$, the shape of the energy relaxation is, according to the present results, more intrinsic to the glassy state than that of the volume relaxation. However, if the shape appears universal, the typical relaxation time τ strongly depends on composition. In particular, relaxation has been shown to be fastest for isostatic systems, which are characterized by an atomic network rigid but free of internal stress [43, 47]. Beyond glasses, being able to predict and tune the relaxation and aging of materials could improve the understanding of memory encoded materials [48, 49] or protein folding [50, 51].

The authors acknowledge financial support for this research provisioned by the University of California, Los Angeles (UCLA). GNS acknowledges the National Science Foundation (CAREER: 1253269) for partial support of this work.

* Contact: bauchy@ucla.edu;

Homepage: <http://mathieu.bauchy.com>

- [1] E. D. Zanotto, *American Journal of Physics* **66**, 392 (1998).
- [2] E. D. Zanotto and P. K. Gupta, *American Journal of Physics* **67**, 260 (1999).
- [3] Y. M. Stokes, *Proceedings of the Royal Society of London A: Mathematical, Physical and Engineering Sciences* **455**, 2751 (1999).
- [4] R. Welch, J. Smith, M. Potuzak, X. Guo, B. Bowden, T. Kiczanski, D. Allan, E. King, A. Ellison, and J. Mauro, *Physical Review Letters* **110**, 265901 (2013).
- [5] M. Vannoni, A. Sordini, and G. Molesini, *Optics Express* **18**, 5114 (2010).
- [6] B. Ruta, G. Baldi, Y. Chushkin, B. Rufflé, L. Cristofolini, A. Fontana, M. Zanatta, and F. Nazzani, *Nature Communications* **5** (2014), 10.1038/ncomms4939.
- [7] R. Sahu, A. K. Gangopadhyay, K. F. Kelton, S. Chatterjee, and K. L. Sahoo, *Scripta Materialia* **61**, 588 (2009).
- [8] C. R. Kurkjian and W. R. Prindle, *Journal of the American Ceramic Society* **81**, 795 (1998).
- [9] A. Bunde, K. Funke, and M. D. Ingram, *Solid State Ionics* **105**, 1 (1998).
- [10] J. C. Phillips, *Reports on Progress in Physics* **59**, 1133 (1996).
- [11] G. Yang, J.-C. Sangleboeuf, C. Boussard-Plédel, and B. Bureau, *Journal of the American Ceramic Society* **96**, 464 (2013).
- [12] J. C. Mauro, D. C. Allan, and M. Potuzak, *Physical Review B* **80**, 094204 (2009).
- [13] A. Tandia, K. D. Vargheese, J. C. Mauro, and A. K. Varshneya, *Journal of Non-Crystalline Solids* **358**, 316 (2012).
- [14] S. Plimpton, *Journal of computational physics* **117**, 1 (1995).
- [15] A. N. Cormack, J. Du, and T. R. Zeitler, *Phys. Chem. Chem. Phys.* **4**, 3193 (2002).
- [16] M. Bauchy, *The Journal of Chemical Physics* **137**, 044510 (2012).
- [17] M. Bauchy, B. Guillot, M. Micoulaut, and N. Sator, *Chemical Geology* **346**, 47 (2013).
- [18] Y. Xiang, J. Du, M. M. Smedskjaer, and J. C. Mauro, *The Journal of Chemical Physics* **139**, 044507 (2013).
- [19] J. A. N. Zasadzinski, *Journal of Microscopy* **150**, 137 (1988).
- [20] J. Du, in *Molecular Dynamics Simulations of Disordered Materials*, Springer Series in Materials Science No. 215, edited by C. Massobrio, J. Du, M. Bernasconi, and P. S. Salmon (Springer International Publishing, 2015) pp. 157–180.
- [21] G. T. Barkema and N. Mousseau, *Physical Review Letters* **77**, 4358 (1996).
- [22] P. Richard, M. Nicodemi, R. Delannay, P. Ribi re, and D. Bideau, *Nature Materials* **4**, 121 (2005).
- [23] R. M bius and C. Heussinger, *Soft Matter* **10**, 4806 (2014).
- [24] D. J. Lacks, *Physical Review Letters* **87**, 225502 (2001).
- [25] D. J. Lacks and M. J. Osborne, *Physical Review Letters* **93**, 255501 (2004).
- [26] M. Utz, P. G. Debenedetti, and F. H. Stillinger, *Physical Review Letters* **84**, 1471 (2000).
- [27] A. V. Lyulin and M. A. J. Michels, *Physical Review Letters* **99**, 085504 (2007).
- [28] J. Rottler and M. Warren, *The European Physical Journal Special Topics* **161**, 55 (2008).
- [29] D. Bonn, S. Tanase, B. Abou, H. Tanaka, and J. Meunier, *Physical Review Letters* **89**, 015701 (2002).
- [30] V. Viasnoff and F. Lequeux, *Physical Review Letters* **89**, 065701 (2002).
- [31] N. V. Priezjev, *Physical Review E* **87**, 052302 (2013).
- [32] D. Fiocco, G. Foffi, and S. Sastry, *Physical Review E* **88**, 020301 (2013).
- [33] M. Parrinello and A. Rahman, *Journal of Applied Physics* **52**, 7182 (1981).
- [34] G. H. Vineyard, *Journal of Physics and Chemistry of Solids* **3**, 121 (1957).
- [35] E. Masoero, H. Manzano, E. Del Gado, R. J. M. Pellenq, F. J. Ulm, and S. Yip, *Mechanics and Physics of Creep, Shrinkage, and Durability of Concrete: A Tribute to Zdenk P. Bazant*, 166 (2013).
- [36] M. Potuzak, R. C. Welch, and J. C. Mauro, *The Journal of Chemical Physics* **135**, 214502 (2011).
- [37] S. I. Simdyankin and N. Mousseau, *Physical Review E* **68**, 041110 (2003).
- [38] S. Bhosle, K. Gunasekera, P. Chen, P. Boolchand, M. Micoulaut, and C. Massobrio, *Solid State Communications* **151**, 1851 (2011).
- [39] C. A. Angell, Y. Yue, L.-M. Wang, J. R. D. Copley, S. Borick, and S. Mossa, *Journal of Physics: Condensed Matter* **15**, S1051 (2003).
- [40] Y. Z. Yue, S. L. Jensen, and J. d. Christiansen, *Applied*

- Physics Letters **81**, 2983 (2002).
- [41] J. C. Mauro and M. M. Smedskjaer, *Physica A: Statistical Mechanics and its Applications* **391**, 6121 (2012).
- [42] J. C. Mauro and M. M. Smedskjaer, *Physica A: Statistical Mechanics and its Applications* **391**, 3446 (2012).
- [43] M. Bauchy and M. Micoulaut, *Nature Communications* **6** (2015), 10.1038/ncomms7398.
- [44] M. Bauchy and M. Micoulaut, *Physical Review B* **83**, 184118 (2011).
- [45] M. J. Abdolhosseini Qomi, M. Bauchy, F.-J. Ulm, and R. J.-M. Pellenq, *The Journal of Chemical Physics* **140**, 054515 (2014).
- [46] N. Mousseau, arXiv:cond-mat/0004356 (2000), arXiv:cond-mat/0004356.
- [47] S. Chakravarty, D. G. Georgiev, P. Boolchand, and M. Micoulaut, *Journal of Physics: Condensed Matter* **17**, L1 (2005).
- [48] D. Fiocco, G. Foffi, and S. Sastry, *Physical Review Letters* **112**, 025702 (2014).
- [49] D. Fiocco, G. Foffi, and S. Sastry, arXiv:1503.00478 [cond-mat] (2015), arXiv: 1503.00478.
- [50] N. Mousseau, P. Derreumaux, G. T. Barkema, and R. Malek, *Journal of Molecular Graphics and Modelling* **19**, 78 (2001).
- [51] J. C. Phillips, *Physical Review E* **80** (2009), 10.1103/PhysRevE.80.051916.